Electronic Supplementary Material (ESI) for Inorganic Chemistry Frontiers.

Supplemental Information File

Synthesis of Chiral High-Entropy Sulfides for the Non-Linear Optical Applications

Nethmi W. Hewage[1,2], Gayatri Viswanathan[1,2], Philip Yox[1,2], Kui Wu[3], Kirill Kovnir[1,2,*] Georgiy Akopov[1,2,4,*]

[1] *Department of Chemistry, Iowa State University, Ames, IA 50011, United States.*

[2] *Ames National Laboratory, U.S. Department of Energy, Ames, IA 50011, United States.*

[3] *State Key Laboratory of Crystal Materials and Institute of Crystal Materials, Shandong University, Jinan, 071002 China.*

[4] *Department of Chemistry, Rutgers University - Newark, Newark, NJ 07102, United States.*

*Corresponding authors: kovnir@iastate.edu, georgiy.akopov@rutgers.edu

Experimental Methods

Synthesis

Materials used: S powder (99.5%, Alfa Aesar, USA); Cu, Mn, Y, La, Ce, Sm, and Gd as well as Ge pieces were acquired from the Materials Preparation Center at Ames Laboratory, which is supported by the US DOE Basic Energy Sciences: Cu pellets (99.995%), Mn pieces (99.99%), Y chunk (99.9999%), La chunk (99.9999%), Ce chunk 99.9999%), Sm chunk (99.9999%), Gd chunk (99.9999%), and Ge lumps (99.999%).

Precursors: Precursors with overall composition $(A)_6(TM)Ge_2S_{14}$ (*A* = La, Sm, Gd, *HEA* = YLaCeSmGd, *TM* = Mn, Cu) were prepared using pieces of appropriate metals and germanium. Samples with a total mass of 0.6 – 1.0 g were weighed out in a ratio of *RE*:Mn:Ge = 6:1:2.1, *RE*:Cu:Ge = 6:2:2.1, *RE*:Mn:Cu:Ge = 6:0.5:1:2.1 and arc-melted. Details of the arc-melting procedure can be found elsewhere.[1]

Bulk powders of the materials were synthesized using the appropriate arc-melted precursor and sulfur powder. Samples were prepared by loading the finely ground precursor and sulfur (1:14 molar ratio) in a fused silica ampoule, which was then flame sealed under vacuum. The samples were heated over 12 hours to 1050°C, dwelled for 72-120 hours, and then cooled to room temperature over 8 hours. Samples with high-entropy compositions were ground in an agate mortar and re-annealed one more time using the same synthesis profile to achieve homogeneity.

Single crystals were grown using the pre-arc-melted precursor, S powder, and potassium iodide (KI) salt flux. The ratio of (precursor + S) to KI flux was kept at 1 to 30 by mass (*e.g.* for 0.1g of reactants, 3g of KI was used). The reactants and KI salt were added to a silica ampule, which was then sealed under vacuum. The samples were heated over 12 hours to 1050°C, dwelled for 72-120

hours, and then cooled to room temperature over 8 hours. The reaction products were washed with deionized water to remove the KI flux, and the sample was then vacuum filtered and allowed to dry.

X-ray Diffraction

Powder X-ray diffraction (PXRD) was performed using a Rigaku Miniflex 600 with Cu-K_α radiation and a Ni-K_β filter. Sample holders were composed of zero-background silicon plates. A thin layer of grease was applied to the surface and sample powders were sprinkled on top.

Single crystal X-ray diffraction (SCXRD) was performed using a Bruker D8 Venture diffractometer using Mo-K_α radiation. The crystal datasets were collected at 100 K or 173 K under a stream of dry N_2. All datasets had ω-scans recorded at a 0.3 - 0.6° step width and were integrated with the Bruker SAINT software package. Structure determination and refinement of the crystal structures were carried out using the SHELX suite of programs.[2] Transition metal site occupancies were refined. For Mn-Cu structures the occupancies of Mn and Cu were refined independently. The rare-earth metal site occupancies for *HEA* compositions were set at 20% per lanthanide and not further refined with constraints of atomic coordinates and atomic displacement parameters set to be equal for all lanthanides.

Scanning Electron Microscopy/Energy Dispersive Spectroscopy (SEM/EDS)

Elemental analysis of samples was conducted using a FEI Quanta 250 field emission-SEM with EDS detector (Oxford X-Max 80, ThermoFischer Scientific, Inc., USA) and analyzed using the Aztec software. Powder samples were mounted in epoxy, polished to a level surface, and coated with a conductive layer of carbon. An accelerating voltage of 15kV was used to study all samples.

Solid-State Diffuse Reflectance Spectroscopy

The UV/Vis diffuse reflectance spectra were measured from 200-1080 nm with a BLACK-Comet C-SR-100 spectrometer. Powder samples were finely ground and flattened on a microscope slide. Band gaps were estimated through extrapolation of the linear slope in the corresponding Tauc plots by plotting $(A\textit{hv})^{1/r}$ vs $\textit{hv}$ where r = ½ for direct and r = 2 for indirect band gaps.

Second Harmonic Generation (SHG) and Laser Damage Threshold (LDT)

Through the Kurtz and Perry method, powder SHG responses were investigated by a *Q*-switch laser (2.09 μm, 3 Hz, 50 ns) with different particle sizes, including 38-55, 55-88, 88-105, 105-150, 150-200, and 200-250 μm. The $AgGaS_2$ single crystal was ground and sieved into the same size range as the reference. The LDTs were evaluated on powder sample (38-55 μm) with a pulsed YAG laser. A similar particle size of $AgGaS_2$ was chosen as the reference. To adjust different laser beams, an optical concave lens is added into the laser path. The damage spot is measured by the scale of an optical microscope.

Table S1A. SCXRD data collection and refinement parameters for $(A)_6(TM)Ge_2S_{14}$ compositions (*A* = La, Sm, Gd, *HEA* = YLaCeSmGd, *TM* = Mn, Cu).

Phase	**$La_6MnGe_2S_{14}$**	**$Sm_6MnGe_2S_{14}$**	**$Gd_6MnGe_2S_{14}$**	**$(HEA)_{1.2}MnGe_2S_{14}$**	**$(HEA)_6Cu_2Ge_2S_{14}$**
CSD-number	2266452	2266458	2266460	2266455	2266456
Space group	$P6_3$				
λ (Å)	Mo-K_α: 0.71073				
***T* (K)**	100(2)	100(2)	100(2)	100(2)	100(2)
***a* (Å)**	10.3659(4)	10.0192(5)	9.9310(4)	10.1513(4)	10.1311(4)
***c* (Å)**	5.8005(3)	5.7239(4)	5.7198(3)	5.7674(3)	5.8113(3)
***V* (Å^{-3})**	539.77(5)	497.61(6)	488.54(5)	514.70(5)	516.56(5)
Z	1				
ρ (g•cm^{-3})	4.555	5.176	5.413	4.697	4.904
Absorption correction	multi-scan				
μ (mm^{-1})	16.217	22.433	25.183	20.365	21.653
θ (°)	$2.27 < \theta < 33.13$	$2.34 < \theta < 33.17$	$2.37 < \theta < 33.28$	$2.32 < \theta < 33.39$	$4.02 < \theta < 33.25$
Data / param.	1374 / 39	1282 / 38	1266 / 39	1342 / 39	1317 / 39
R_1	0.013	0.036	0.020	0.016	0.016
wR_2	0.025	0.050	0.032	0.029	0.026
Goodness-of-fit	1.05	0.96	1.05	1.06	1.06
Flack Param.	0.03(2)	0.05(3)	0.03(2)	0.06(2)	0.06(1)
Diff. peak/hole (e•Å^{-3})	0.36 / -0.60	1.91 / -2.14	1.08 / -1.19	0.94 / -0.85	0.68 / -0.86

Table S1B. SCXRD data collection and refinement parameters for $(A)_6(TM)Ge_2S_{14}$ compositions (*A* = La, Sm, Gd, *HEA* = YLaCeSmGd, *TM* = Mn, Cu).

Phase	**$La_6Mn_{0.5}CuGe_2S_{14}$**	**$Sm_6Mn_{0.5}CuGe_2S_{14}$**	**$Gd_6Mn_{0.5}CuGe_2S_{14}$**	**$(HEA)_{1.2}Mn_{0.5}CuGe_2S_{14}$**	**$(HEA)_{1.2}Mn_{0.5}CuGe_2S_{14}$**
CSD-number	2266451	2266454	2266459	2266457	2266453
Space group	$P6_3$				
λ (Å)	Mo-K_α: 0.71073				
***T* (K)**	100(2)	173(2)	173(2)	100(2)	173(2)
***a* (Å)**	10.3374(4)	10.0219(3)	9.9448(4)	10.1366(4)	10.1882(3)
***c* (Å)**	5.8457(3)	5.7484(3)	5.7333(3)	5.7986(3)	5.7979(3)
***V* (Å^{-3})**	540.99(5)	500.01(4)	491.05(5)	515.99(5)	521.19(4)
Z	1				
ρ (g•cm^{-3})	4.712	5.275	5.491	4.850	4.728
Absorption correction	multi-scan				
μ (mm^{-1})	17.192	23.100	25.719	21.300	20.649
θ (°)	$3.94 < \theta < 33.08$	$2.35 < \theta < 33.19$	$2.37 < \theta < 33.13$	$4.02 < \theta < 33.27$	$2.31 < \theta < 33.44$
Data / param.	1367 / 43	1283 / 43	1262 / 43	1317 / 43	1362 / 43
R_1	0.016	0.018	0.012	0.017	0.027
wR_2	0.027	0.029	0.024	0.027	0.041
Goodness-of-fit	1.05	1.08	1.07	1.07	1.04
Flack Param.	0.04(2)	0.04(2)	0.03(1)	0.05(1)	0.10(2)
Diff. peak/hole (e•Å^{-3})	0.78 / -0.75	0.87 / -1.18	0.75 / -0.61	0.68 / -0.73	1.30 / -1.23

Table S2A. Crystallographic data for $(A)_6MnGe_2S_{14}$ phases (*A* = La, Sm, Gd, *HEA* = YLaCeSmGd) and selected bond lengths, angles, and volumes of the space filling octahedra.

Parameter	$La_6MnGe_2S_{14}$	$Sm_6MnGe_2S_{14}$	$Gd_6MnGe_2S_{14}$	$(HEA)_6MnGe_2S_{14}$
$r(Ln)_{ionic}$ [a]	1.160	1.079	1.053	1.091 [b]
***a* (Å)**	10.3659(4)	10.0192(5)	9.9310(4)	10.1513(4)
***c* (Å)**	5.8005(3)	5.7239(4)	5.7198(3)	5.7674(3)
***V* (Å^3)**	539.78	497.61	488.54	514.70
$[LnS_8]$				
d(*Ln*-S) (Å)	2.883-3.139	2.786-3.125	2.759-2.315	2.826-3.145
$d(Ln\text{-}S)_{mean}$ (Å)	3.001	2.916	2.899	2.951
V (Å^3)	46.77	42.93	42.13	44.51
$[GeS_4]_{Td}$				
d(Ge1-S3) (Å)	2.227	2.220	2.221	2.227
d(Ge1-S1) (Å) [c]	2.175	2.171	2.168	2.174
$d(Ge\text{-}S)_{mean}$ (Å) [d]	2.214	2.208	2.208	2.214
Δd(Ge-S) (%) [e]	2.33	2.21	2.39	2.38
∠ S3-Ge-S1 (º)	112.706	113.535	113.848	113.226
∠ S3-Ge-S3 (º)	106.052	105.119	104.762	105.424
V_{Td} (Å^3)	5.55	5.49	5.48	5.53
$[MnS_6]_{Oh}$				
d(Mn-S) (Å)	2.668-2.680	2.613-2.637	2.603-2.628	2.643-2.654
$d(Mn\text{-}S)_{mean}$ (Å)	2.674	2.625	2.616	2.648
Δd(Mn-S) (%) [e]	0.45	0.91	0.95	0.41
$(\angle S2\text{-}Mn1\text{-}S2)_{axial}$ (º)	179.582	179.204	179.161	179.623
$(\angle S2\text{-}Mn1\text{-}S2)_{equat}$ (º)	86.630	86.889	87.032	86.828
V_{Oh} (Å^3)	25.35	24.01	23.76	24.64

[a] from Shannon [3];
[b] ionic radius for the *HEA* composition was calculated as the average of Y, La, Ce, Sm and Gd ionic radii;
[c] Ge-S bond along the [001] direction;
[d] mean interatomic distance;
[e] difference between actual and mean bond lengths.

Table S2B. Crystallographic data for $(A)_6(TM)Ge_2S_{14}$ phases (*A* = La, Sm, Gd, *HEA* = YLaCeSmGd, *TM* = Mn, Cu) and selected bond lengths, angles, and volumes of the space filling octahedra.

Parameter	$La_6Mn_{0.5}CuGe_2S_{14}$	$Sm_6Mn_{0.5}CuGe_2S_{14}$	$Gd_6Mn_{0.5}CuGe_2S_{14}$	$(HEA)_6Cu_2Ge_2S_{14}$
$r(Ln)_{ionic}$ [a]	1.160	1.079	1.053	1.091 [b]
***a* (Å)**	10.3374(4)	10.0119(3)	9.9448(4)	10.1311(4)
***c* (Å)**	5.8457(3)	5.7462(2)	5.7333(3)	5.8113(3)
***V* (Å^3)**	540.99	498.82	491.05	516.56
$[LnS_8]$				
d(*Ln*-S) (Å)	2.879-3.156	2.791-3.125	2.769-3.139	2.829-3.153
$d(Ln\text{-}S)_{mean}$ (Å)	3.004	2.919	2.903	2.956
V (Å^3)	46.97	43.09	42.38	44.77
$[GeS_4]_{Td}$				
d(Ge1-S3) (Å)	2.226	2.219	2.223	2.224
d(Ge1-S1) (Å) [c]	2.179	2.172	2.171	2.179
$d(Ge\text{-}S)_{mean}$ (Å) [d]	2.214	2.207	2.210	2.213
Δd(Ge-S) (%) [e]	2.11	2.12	2.34	2.02
∠ S3-Ge-S1 (º)	112.890	113.707	113.900	113.496
∠ S3-Ge-S3 (º)	105.846	104.923	104.701	105.163
V_{Td} (Å^3)	5.54	5.48	5.50	5.52
$[MnS_6]_{Oh}$				
d(Mn-S) (Å)	2.697 - 2.700	2.649 – 2.653	2.640 – 2.645	-
$d(Mn\text{-}S)_{mean}$ (Å)	2.698	2.615	2.642	-
Δd(Mn-S) (%) [e]	0.11	0.15	0.19	-
$(\angle S2\text{-}Mn1\text{-}S2)_{axial}$ (º)	179.875	179.875	179.854	-
$(\angle S2\text{-}Mn1\text{-}S2)_{equat}$ (º)	86.559	86.585	86.636	-
V_{Oh} (Å^3)	26.05	24.7	24.47	-
$[CuS_3]_{\Delta}$				
d(Cu-S) (Å)	2.269	2.229	2.222	2.265
α (∠ **Cu1-Cu1-S2) (º)**	88.391	92.038	92.351	92.309
β (∠ **S2-Cu1-S2) (º)**	119.922	119.875	119.833	119.839

[a] from Shannon [3];
[b] ionic radius for the *HEA* composition was calculated as the average of Y, La, Ce, Sm and Gd ionic radii;
[c] Ge-S bond along the [001] direction;
[d] mean interatomic distance;
[e] difference between actual and mean bond lengths.

Table S2C. Crystallographic data for $(HEA)_6Mn_{0.5}CuGe_2S_{14}$ phases (*HEA* = YLaCeSmGd) and select bond lengths, angles, and volumes of the space filling octahedra.

Parameter	$(HEA)_6Mn_{0.5}CuGe_2S_{14}$	$(HEA)_6Mn_{0.5}CuGe_2S_{14}$
$r(Ln)_{ionic}$ [a]	1.091 [b]	1.091 [b]
a (Å)	10.1366(4)	10.1882(3)
c (Å)	5.7986(3)	5.7979(3)
V (Å^3)	515.99	521.19
$[LnS_8]$		
d(Ln-S) (Å)	2.826-3.153	2.839-3.150
d(Ln-S)$_{mean}$ (Å)	2.954	2.965
V (Å^3)	44.68	45.12
$[GeS_4]_{Td}$		
d(Ge1-S3) (Å)	2.226	2.225
d(Ge1-S1) (Å)[c]	2.178	2.180
d(Ge-S)$_{mean}$ (Å)[d]	2.214	2.214
Δd(Ge-S) (%)[e]	2.16	2.02
∠ S3-Ge-S1 (º)	113.423	113.218
∠ S3-Ge-S3 (º)	105.247	105.478
V_{Td} (Å^3)	5.53	5.54
$[MnS_6]_{Oh}$		
d(Mn-S) (Å)	2.669 – 2.683	2.667 – 2.672
d(Mn-S)$_{mean}$ (Å)	2.676	2.670
Δd(Mn-S) (%)[e]	0.52	0.19
(∠S2-Mn1-S2)$_{axial}$ (º)	179.541	179.833
(∠S2-Mn1-S2)$_{equat}$ (º)	86.578	86.688
V_{Oh} (Å^3)	25.40	25.23
$[CuS_3]_{\Delta}$		
d(Cu-S) (Å)	2.250	2.243
α (∠ Cu1-Cu1-S2) (º)	92.112	91.837
β (∠ S2-Cu1-S2) (º)	119.865	119.898

[a] from Shannon [3];
[b] ionic radius for the *HEA* composition was calculated as the average of Y, La, Ce, Sm and Gd ionic radii;
[c] Ge-S bond along the [001] direction;
[d] mean interatomic distance;
[e] difference between actual and mean bond lengths.

Table S3. Second harmonic generation (SHG) and laser damage threshold (LDT) data for the $(A)_6(TM)Ge_2S_{14}$ compositions (*A* = La, Sm, Gd, *HEA* = YLaCeSmGd, *TM* = Mn, Cu).

Nominal Composition	SHG						LDT		
	Particle Size (μm)						Laser damage energy (mJ)	LDT (MW/cm^2)	LDT (× AGS)
	38-55	55-88	88-105	105-150	150-200	200-250			
$AgGaS_2$ (AGS)	22.4	26.8	28.4	34.4	43.2	47.2	0.58	29.6	1.0
$La_6MnGe_2S_{14}$	18.4	24.8	25.6	33.6	38.4	48.0	1.47	75.0	2.5
$La_6Mn_{0.5}CuGe_2S_{14}$	19.2	24.0	31.2	32.8	35.2	40.8	1.17	59.5	2.0
$Sm_6MnGe_2S_{14}$	28.8	33.6	44.0	48.0	52.0	63.2	1.86	95.0	3.2
$Sm_6Mn_{0.5}CuGe_2S_{14}$[a]	32.0						1.04	53.0	1.8
$Gd_6MnGe_2S_{14}$[a]	40.8						1.18	60.0	2.0
$Gd_6Mn_{0.5}CuGe_2S_{14}$	24.0	29.6	37.6	44.0	48.0	40.0	1.98	101.0	3.4
$(HEA)_{1.2}Cu_2Ge_2S_{14}$	31.2	35.2	39.2	43.2	44.8	63.2	1.63	83.0	2.8
$(HEA)_{1.2}MnGe_2S_{14}$	28.8	30.0	36.0	37.6	42.4	58.0	0.88	45.0	1.5
$(HEA)_{1.2}Mn_{0.5}CuGe_2S_{14}$	19.2	21.6	33.6	35.2	38.4	44.0	1.75	89.2	3.0

[a] not enough material was present to be analyzed at all the different particle sizes.

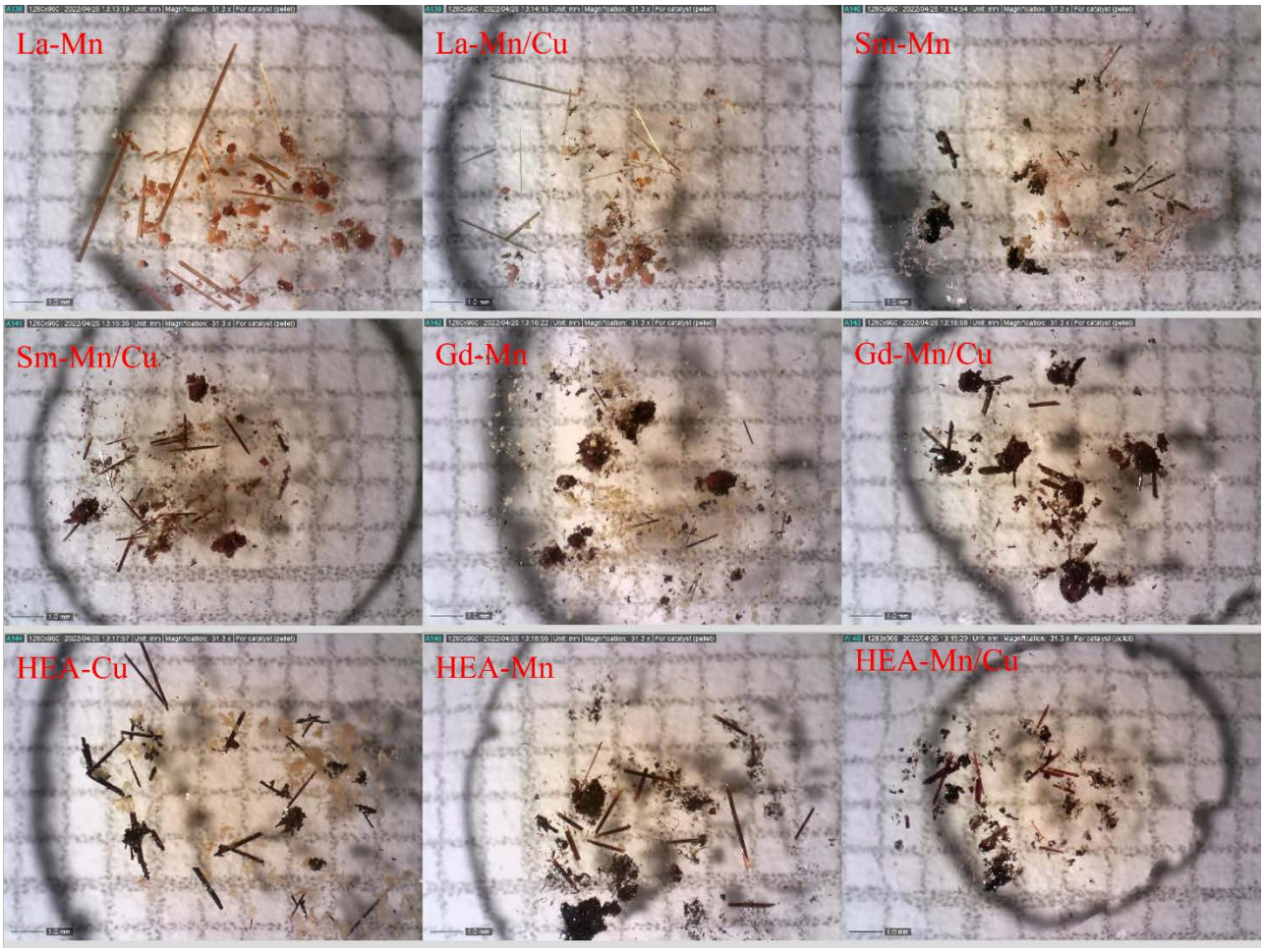

Figure S1. Optical images of the crystals of $(Ln)_6(TM)_xGe_2S_{14}$, where *Ln* = La, Sm, Gd, and HEA (Y+La+Ce+Sm+Gd); *TM* = Mn or $Mn_{0.5}Cu$. Scale bar and grid size are 1 mm in all images.

REFERENCES

(1) Akopov, G.; Hewage, N. W.; Yox, P.; Viswanathan, G.; Lee, S. J.; Hulsebosch, L. P.; Cady, S. D.; Paterson, A. L.; Perras, F. A.; Xu, W.; Wu, K.; Mudryk, Y.; Kovnir, K. Synthesis-Enabled Exploration of Chiral and Polar Multivalent Quaternary Sulfides. *Chem. Sci.* **2021**, *12* (44), 14718–14730. https://doi.org/10.1039/D1SC03685H.

(2) Sheldrick, G. M. A Short History of *SHELX*. *Acta Crystallogr A Found Crystallogr* **2008**, *64* (1), 112–122. https://doi.org/10.1107/S0108767307043930.

(3) Shannon, R. D. Revised Effective Ionic Radii and Systematic Studies of Interatomic Distances in Halides and Chalcogenides. *Acta Cryst A* **1976**, *32* (5), 751–767. https://doi.org/10.1107/S0567739476001551.